Madden-Julian Oscillation: Recent Evolution, Current Status and Predictions

Update prepared by: CPC
Climate Prediction Center / NCEP
5 November 2018

Outline

Overview

Recent Evolution and Current Conditions

MJO Index Information

MJO Index Forecasts

MJO Composites

Overview

- A rapidly eastward-propagating intraseasonal signal transitioned from over Africa to the Indian Ocean during the past week, with a phase speed bordering between an active MJO or Kelvin wave.

- Dynamical RMM index forecasts indicate continued fast propagation of this intraseasonal signal across the Indian Ocean this week (Phases 2/3), and Maritime Continent the following week (Phases 4/5).

- While this intraseasonal signal appears likely to play a key role in the tropical circulation and its associated convection, destructive interference with a suppressed convective signal over the Maritime Continent associated the building El Niño event in the Pacific appears likely during Week-2.

- Also of note is the potential for enhanced tropical cyclone activity in the wake of the eastward-propagating intraseasonal mode over the Indian Ocean during Week-1.

Additional potential impacts across the global tropics and a discussion for the U.S. are available at:
http://www.cpc.ncep.noaa.gov/products/precip/CWlink/ghazards/index.php

850-hPa Vector Wind Anomalies (m s^{-1})

Note that shading denotes the zonal wind anomaly

Blue shades: Easterly anomalies

Red shades: Westerly anomalies

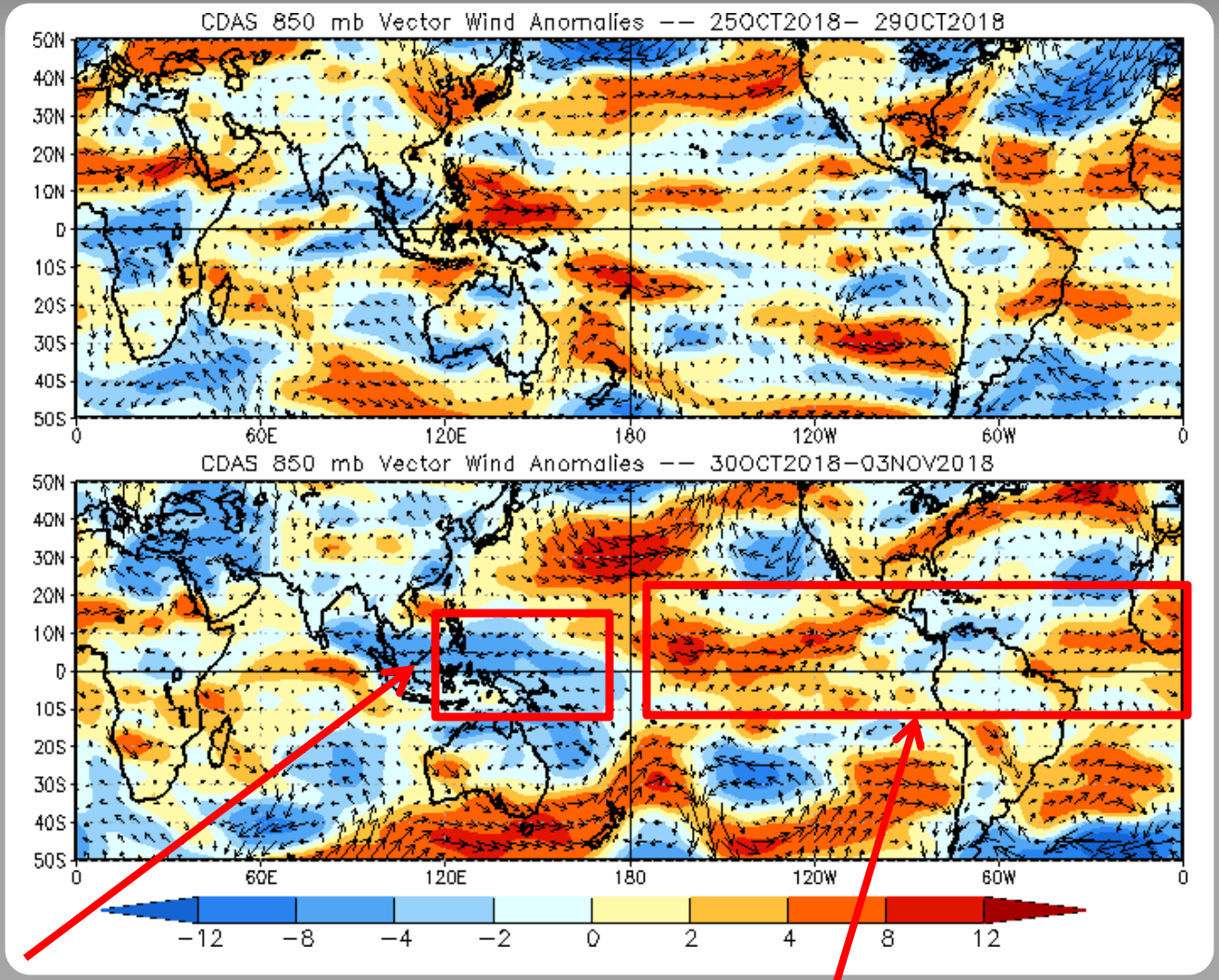

A stark reversal occurred over the West Pacific, with anomalous westerlies reversing to easterlies.

Westerlies persisted over the equatorial eastern Pacific and the tropical North Atlantic.

850-hPa Zonal Wind Anomalies (m s^{-1})

Westerly anomalies (orange/red shading) represent anomalous west-to-east flow

Easterly anomalies (blue shading) represent anomalous east-to-west flow

The MJO was active during May. Westward moving variability weakened the signal in June. A weak intraseasonal signal re-emerged during mid to late July. During August, the intraseasonal signal weakened, and other modes, including Rossby wave and tropical cyclone activity, influenced the pattern.

Through much of September, Rossby wave activity continued in the Pacific, while westerly anomalies overspread the equatorial Pacific with another rapidly propagating intraseasonal feature late in the month.

During September and October, westerly anomalies increased in amplitude and duration over the equatorial Pacific, consistent with a gradual transition towards El Niño conditions. There was signs of another eastward propagating intraseasonal feature from mid-October to early November.

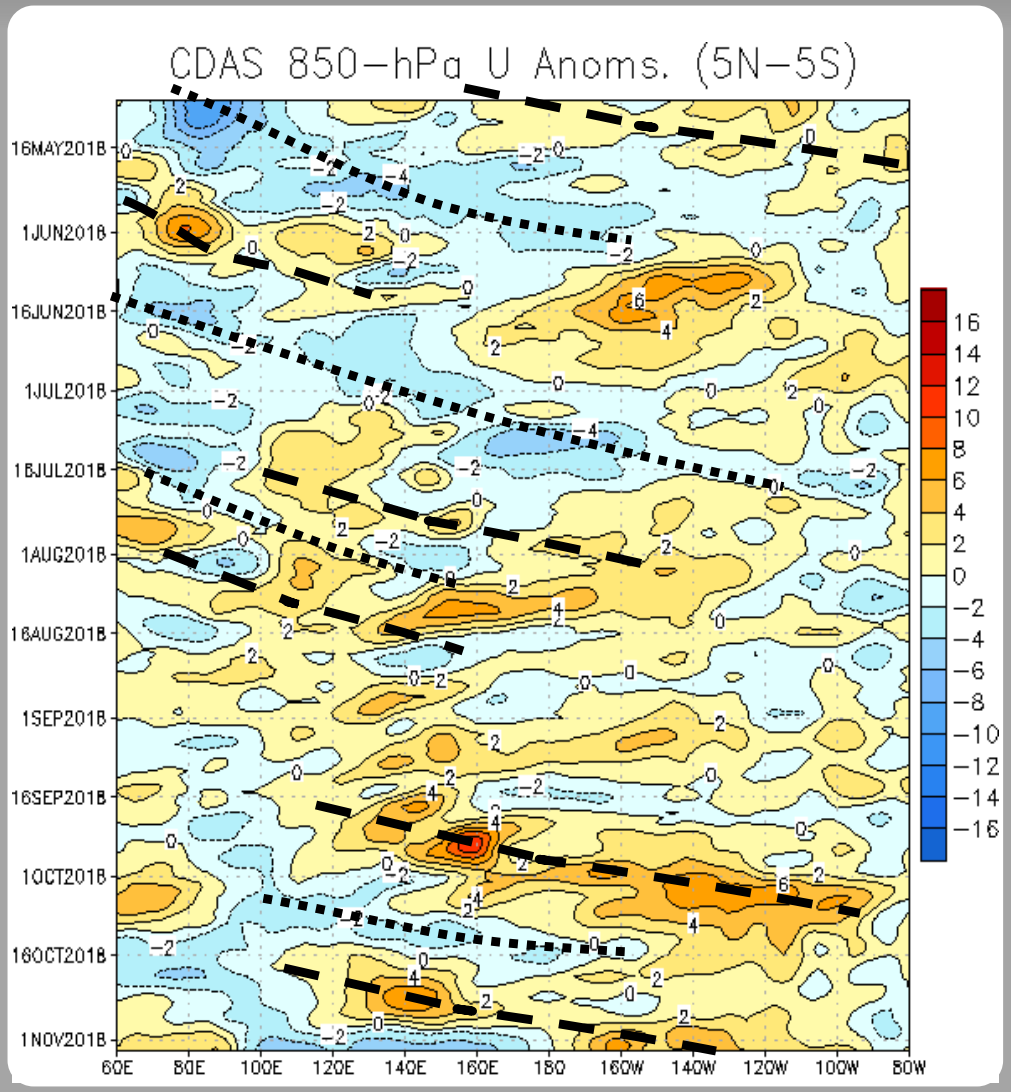

OLR Anomalies – Past 30 days

Drier-than-normal conditions, positive OLR anomalies (yellow/red shading)

Wetter-than-normal conditions, negative OLR anomalies (blue shading)

By early to mid-October, suppressed convection moved over the entire Maritime Continent and parts of the equatorial West and Central Pacific, interfering with the base state. Enhanced convection began building over the western Indian Ocean.

During mid-October, convective anomalies weakened along the equator as the MJO signal began breaking down. A large swath of suppressed convection lifted northward over the South China Sea and the tropical northwestern and central Pacific.

Suppressed convection persisted over the South China Sea, and extended southward over the Western Maritime Continent. Suppressed convection also overspread the Caribbean, noteworthy given this being the typical late-season region for Atlantic TC activity.

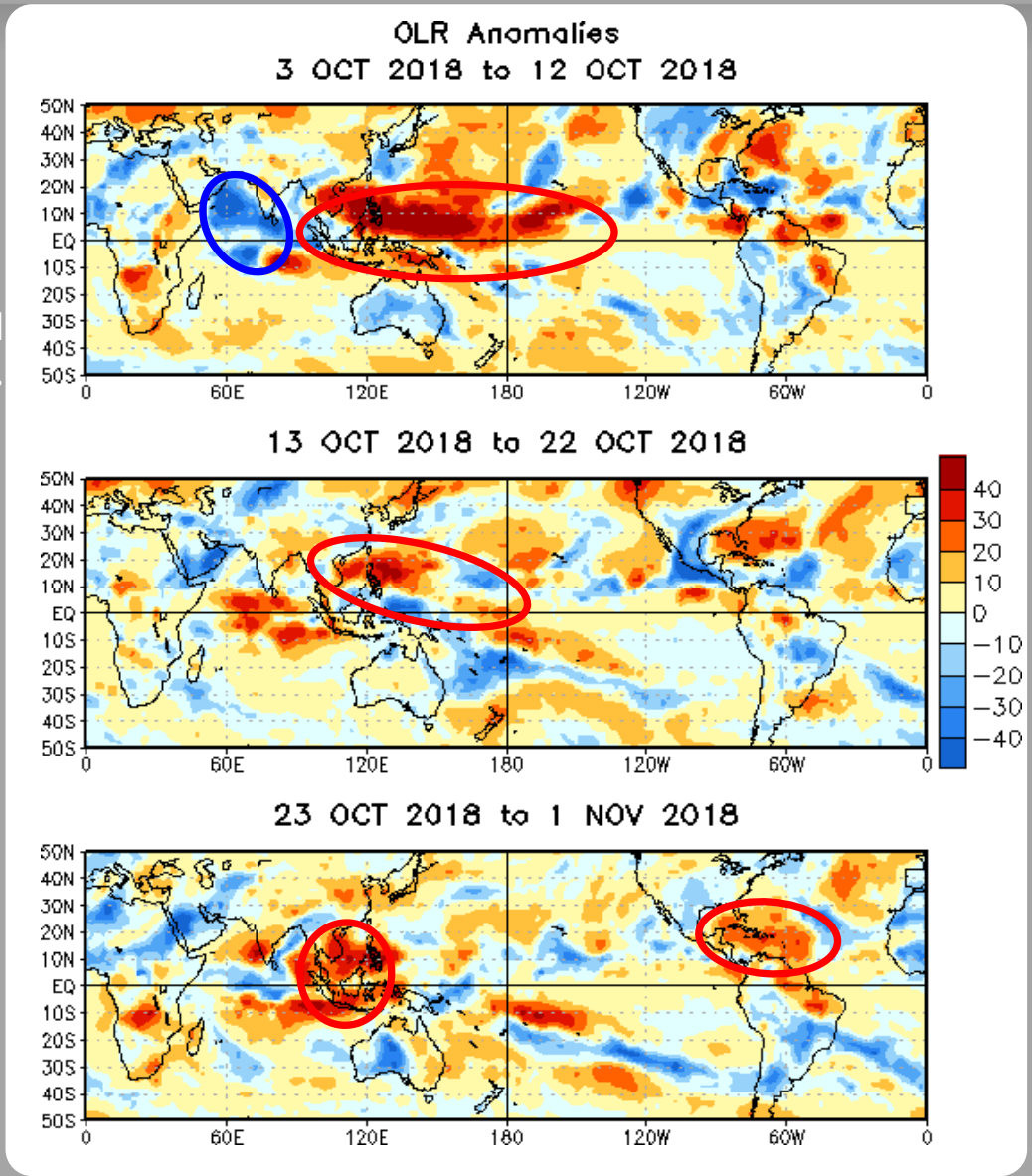

Outgoing Longwave Radiation (OLR) Anomalies (7.5°S - 7.5°N)

Drier-than-normal conditions, positive OLR anomalies (yellow/red shading)

Wetter-than-normal conditions, negative OLR anomalies (blue shading)

The MJO was active during May. The signal weakened in June, but re-emerged during July.

Kelvin waves, Rossby waves, and tropical cyclones dominated the pattern during August and early September, while the intraseasonal signal remained fairly weak.

During mid-September, the suppressed phase of the MJO emerged over the Eastern Indian Ocean and Maritime Continent. During early October, the suppressed signal propagated further east and enhanced convection emerged over the western Indian Ocean.

More recently, the intraseaonal signal weakened, though weak convection has developed over the far western Pacific east of 120° E.

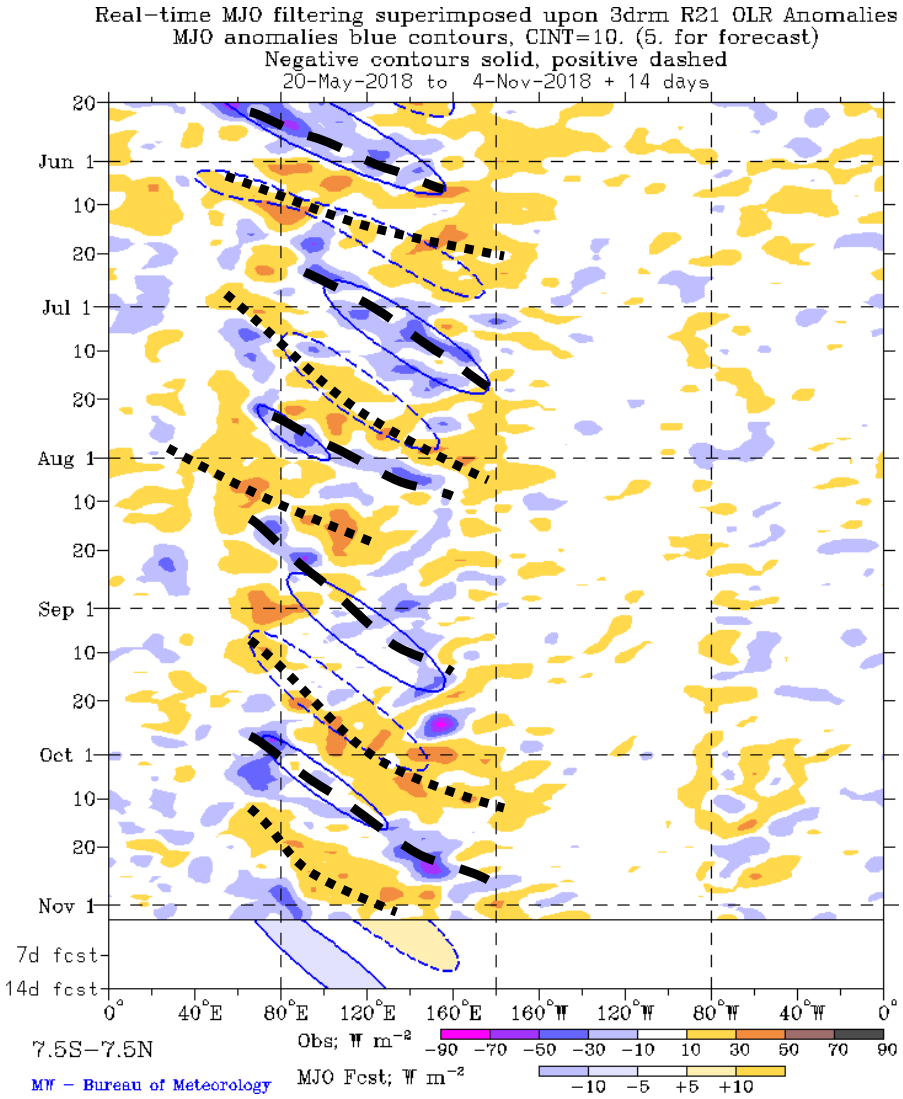

200-hPa Velocity Potential Anomalies (5°S - 5°N)

Positive anomalies (brown shading) indicate unfavorable conditions for precipitation

Negative anomalies (green shading) indicate favorable conditions for precipitation

There was robust MJO activity through boreal spring along with the decay of La Niña conditions. The enhanced phase of the MJO weakened east of the Date Line during June. Eastward propagation of broad suppressed convection continued into early July.

The upper-level footprint of the MJO re-emerged during mid-July, with a broad divergent signal propagating from the Maritime Continent to the central Pacific.

Starting in mid-July, a low-frequency dipole favoring enhanced (suppressed) convection over the east-central Pacific (Indian Ocean) emerged, consistent with a gradual transition towards El Niño conditions.

During mid-September, a robust intraseasonal signal constructively interfered with the base state over the Maritime Continent. The MJO signal persisted into October, and destructively interfered with the base state. More recently, upper-level divergence shifted east into the Western Hemisphere.

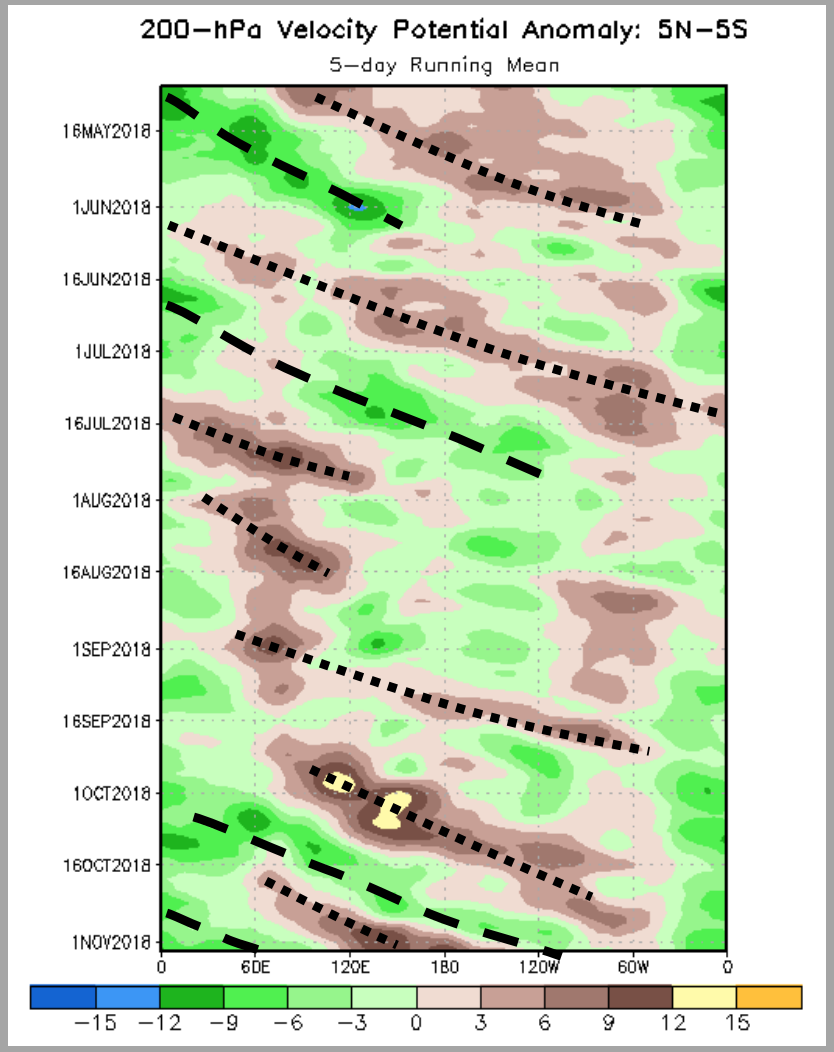

IR Temperatures (K) / 200-hPa Velocity Potential Anomalies

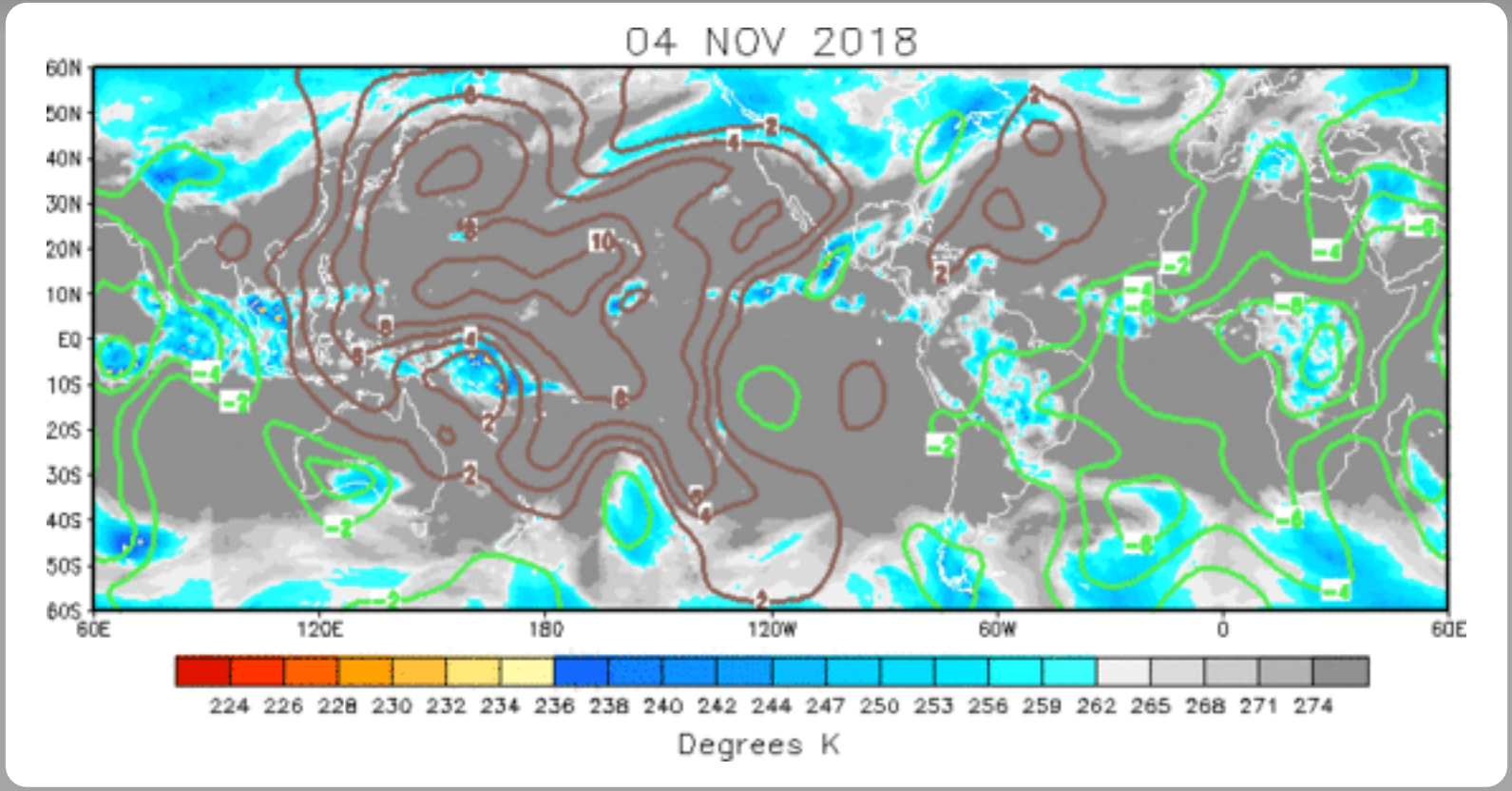

The upper-level velocity potential's spatial pattern featured a wavenumber-1 pattern with enhanced (suppressed) convection over the eastern Atlantic through Indian Ocean (Maritime Continent through Americas, broken up by TC activity over the East Pacific).

Positive anomalies (brown contours) indicate unfavorable conditions for precipitation
Negative anomalies (green contours) indicate favorable conditions for precipitation

200-hPa Vector Wind Anomalies (m s^{-1})

Note that shading denotes the zonal wind anomaly

Blue shades: Easterly anomalies

Red shades: Westerly anomalies

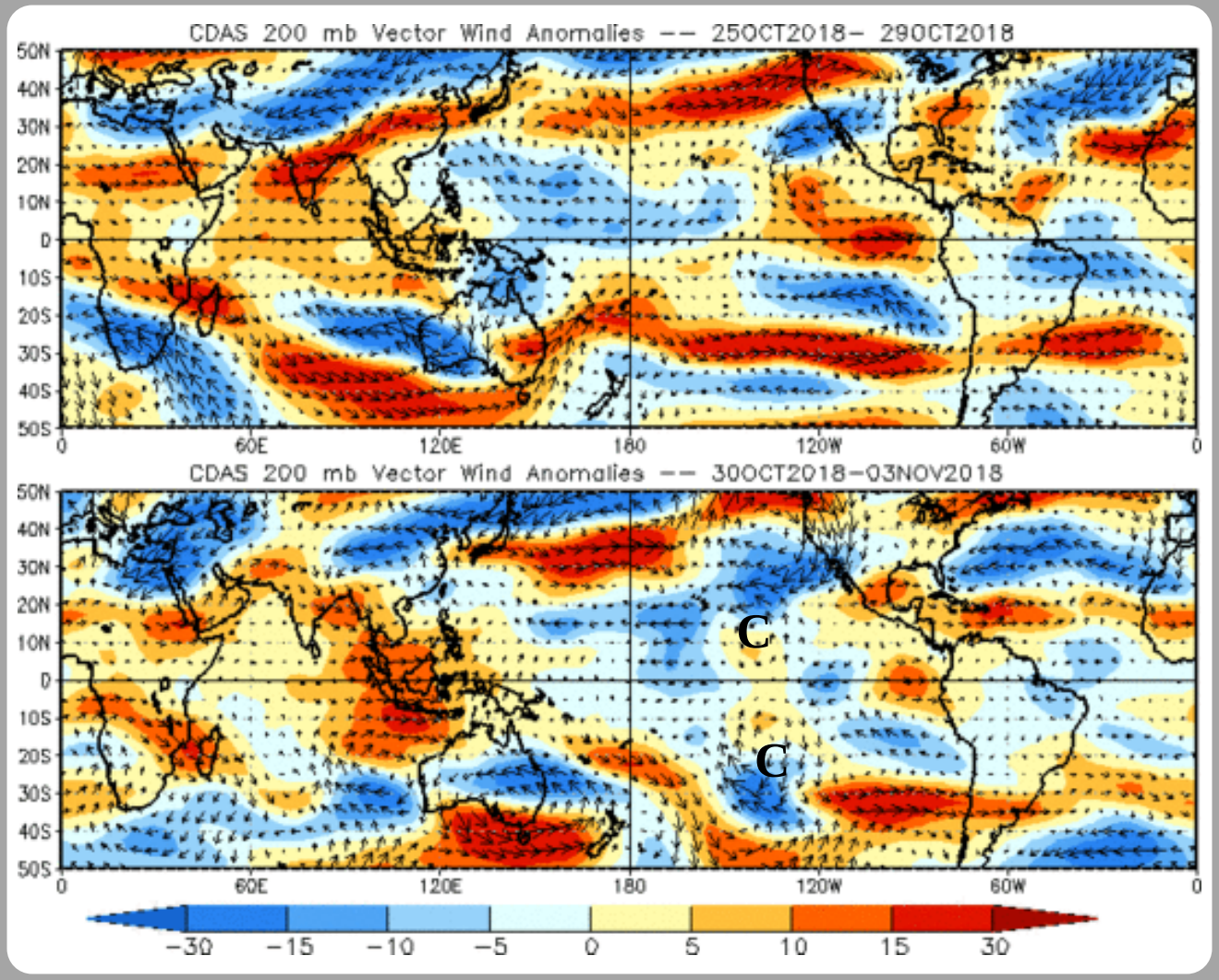

A pair of fairly weak anomalous cyclonic features are apparent off the equator in both hemispheres near 140W.

The upper-level jet extended from Korea through western North America, but was interfered with somewhat by a region of anomalous easterlies associated with an anomalous cyclone over southeast Asia.

200-hPa Zonal Wind Anomalies (m s^{-1})

Westerly anomalies (orange/red shading) represent anomalous west-to-east flow

Easterly anomalies (blue shading) represent anomalous east-to-west flow

Weak westerly anomalies propagated eastward from the Indian Ocean to the Americas in early May; this pattern broke down in early June.

Anomalous westerlies amplified over the Maritime Continent in mid-June and propagated eastward at MJO-like phase speeds.

During August the intraseasonal pattern weakened, with Rossby wave activity influencing the West Pacific pattern.

Anomalous westerlies weakened as they shifted east from the Indian Ocean and into the East Pacific during the past two weeks.

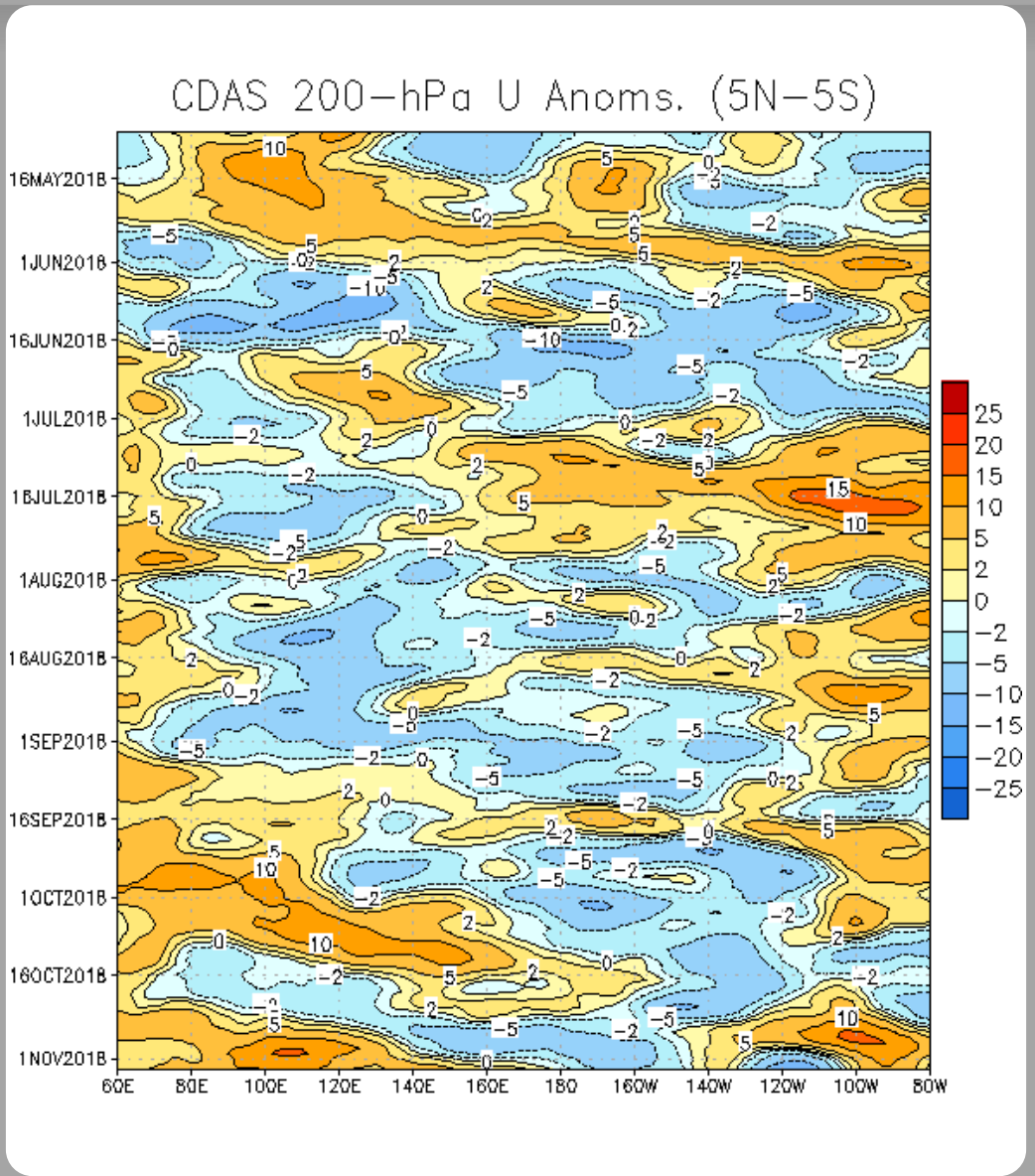

Weekly Heat Content Evolution in the Equatorial Pacific

Oceanic Kelvin waves have alternating warm and cold phases. The warm phase is indicated by dashed lines. Downwelling and warming occur in the leading portion of a Kelvin wave, and upwelling and cooling occur in the trailing portion.

Negative upper-ocean heat content anomalies persisted in the central and eastern Pacific through December.

A downwelling Kelvin wave associated with the intraseasonal signal weakened the negative anomalies across the east-central Pacific during late January and early February.

Several downwelling oceanic Kelvin waves contributed to the eastward expansion of relatively warm subsurface water during February. Positive anomalies have now been observed over most of the basin since April.

The westerly wind burst east of New Guinea in September triggered another oceanic Kelvin wave and round of downwelling, helping to reinforce the warm water availability for a potential El Niño event.

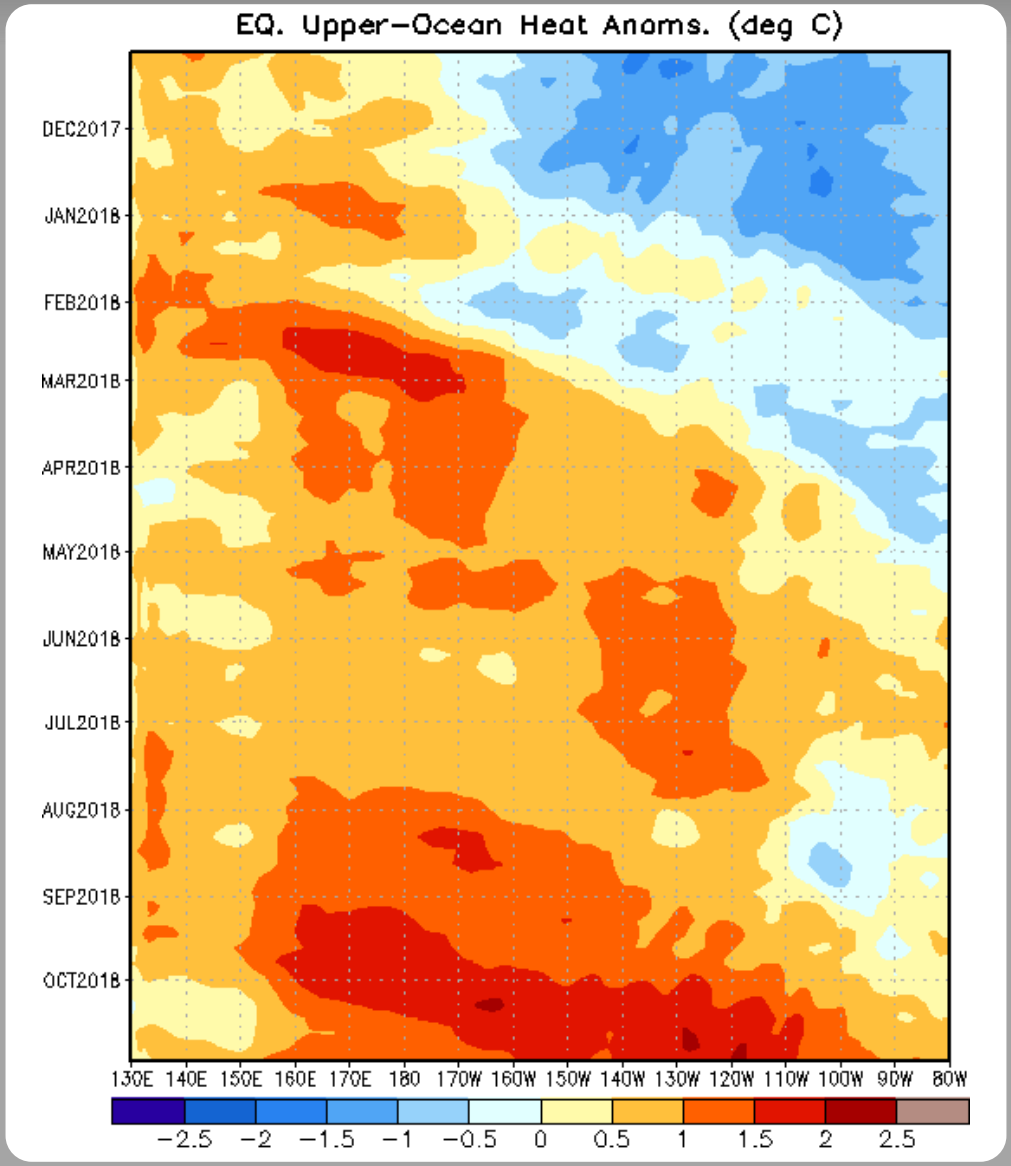

MJO Index -- Information

The MJO index illustrated on the next several slides is the CPC version of the Wheeler and Hendon index (2004, hereafter WH2004).

Wheeler M. and H. Hendon, 2004: An All-Season Real-Time Multivariate MJO Index: Development of an Index for Monitoring and Prediction, *Monthly Weather Review*, 132, 1917-1932.

The methodology is very similar to that described in WH2004 but does not include the linear removal of ENSO variability associated with a sea surface temperature index. The methodology is consistent with that outlined by the U.S. CLIVAR MJO Working Group.

Gottschalck et al. 2010: A Framework for Assessing Operational Madden-Julian Oscillation Forecasts: A CLIVAR MJO Working Group Project, *Bull. Amer. Met. Soc.*, 91, 1247-1258.

The index is based on a combined Empirical Orthogonal Function (EOF) analysis using fields of near-equatorially-averaged 850-hPa and 200-hPa zonal wind and outgoing longwave radiation (OLR).

MJO Index - Recent Evolution

The axes (RMM1 and RMM2) represent daily values of the principal components from the two leading modes

The triangular areas indicate the location of the enhanced phase of the MJO

Counter-clockwise motion is indicative of eastward propagation. Large dot most recent observation.

Distance from the origin is proportional to MJO strength

Line colors distinguish different months

The RMM-based MJO index increased in amplitude during the past week, and propagated eastward toward the Central Indian Ocean.

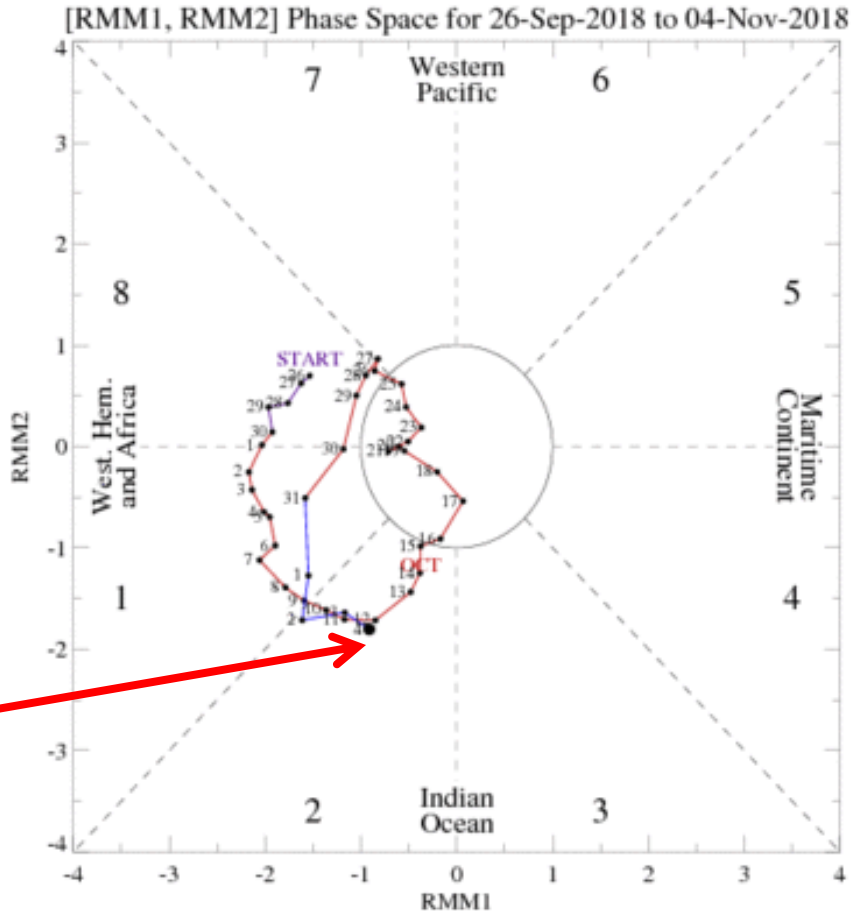

MJO Index - Historical Daily Time Series

Time series of daily MJO index amplitude for the last few years.

Plot puts current MJO activity in recent historical context.

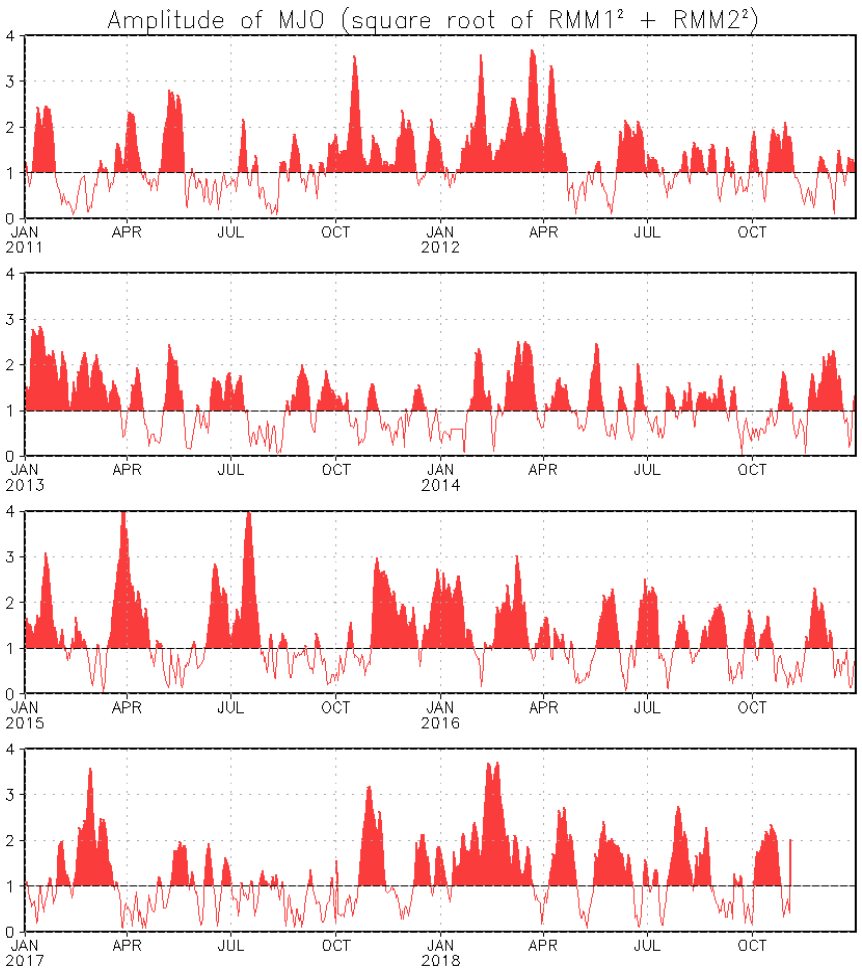

GFS Ensemble (GEFS) MJO Forecast

RMM1 and RMM2 values for the most recent 40 days and forecasts from the GFS ensemble system (GEFS) for the next 15 days

light gray shading: 90% of forecasts

dark gray shading: 50% of forecasts

Yellow Lines - 20 Individual Members
Green Line - Ensemble Mean

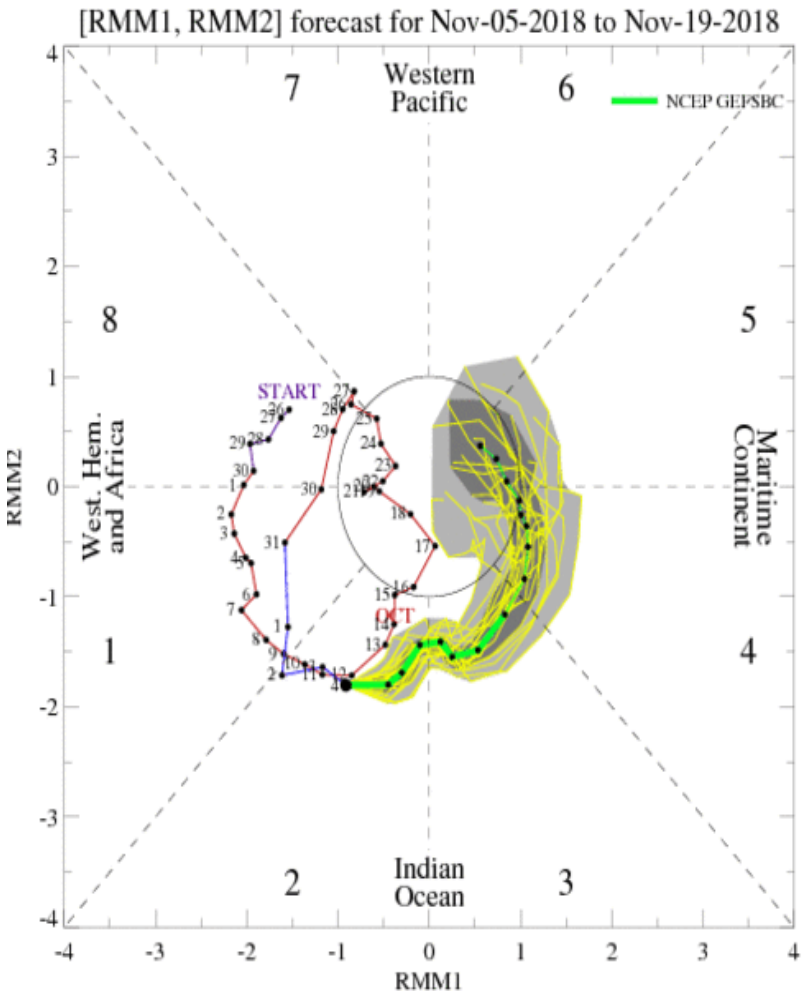

The GEFS-based RMM-index forecast depicts a fast eastward propagation of a signal across the Indian Ocean during the next week, and crossing the Maritime Continent during the following week.

Ensemble GFS (GEFS) MJO Forecast

Figures below show MJO associated OLR anomalies only (reconstructed from RMM1 and RMM2) and do not include contributions from other modes (*i.e.*, ENSO, monsoons, etc.)

Spatial map of OLR anomalies for the next 15 days

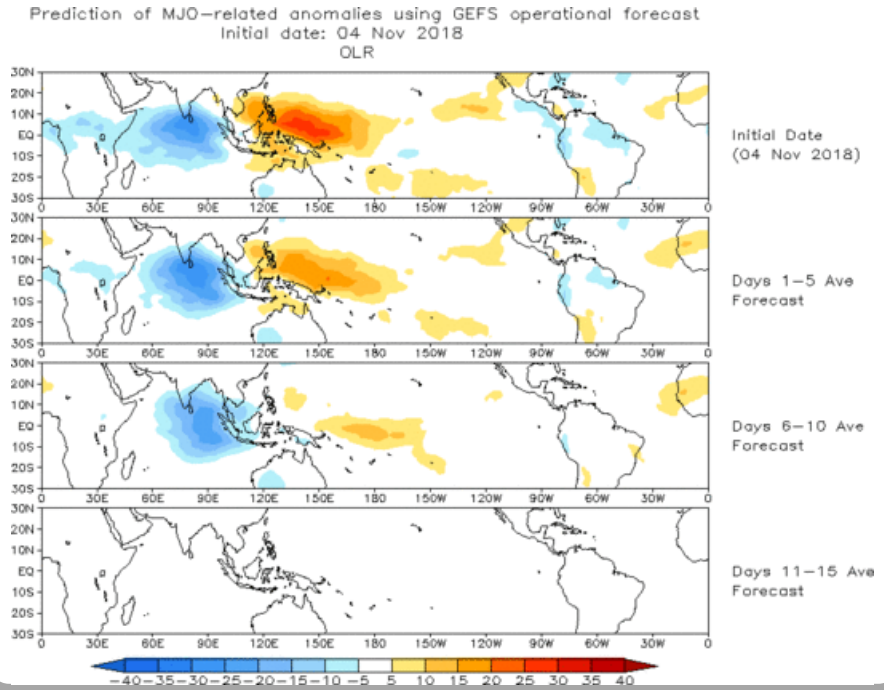

The GEFS RMM-based OLR forecast indicates weakening of the suppressed and active MJO-related convective envelopes during the next 10 days, before these signals become muted.

Time-longitude section of (7.5° S-7.5° N) OLR anomalies - last 180 days and for the next 15 days

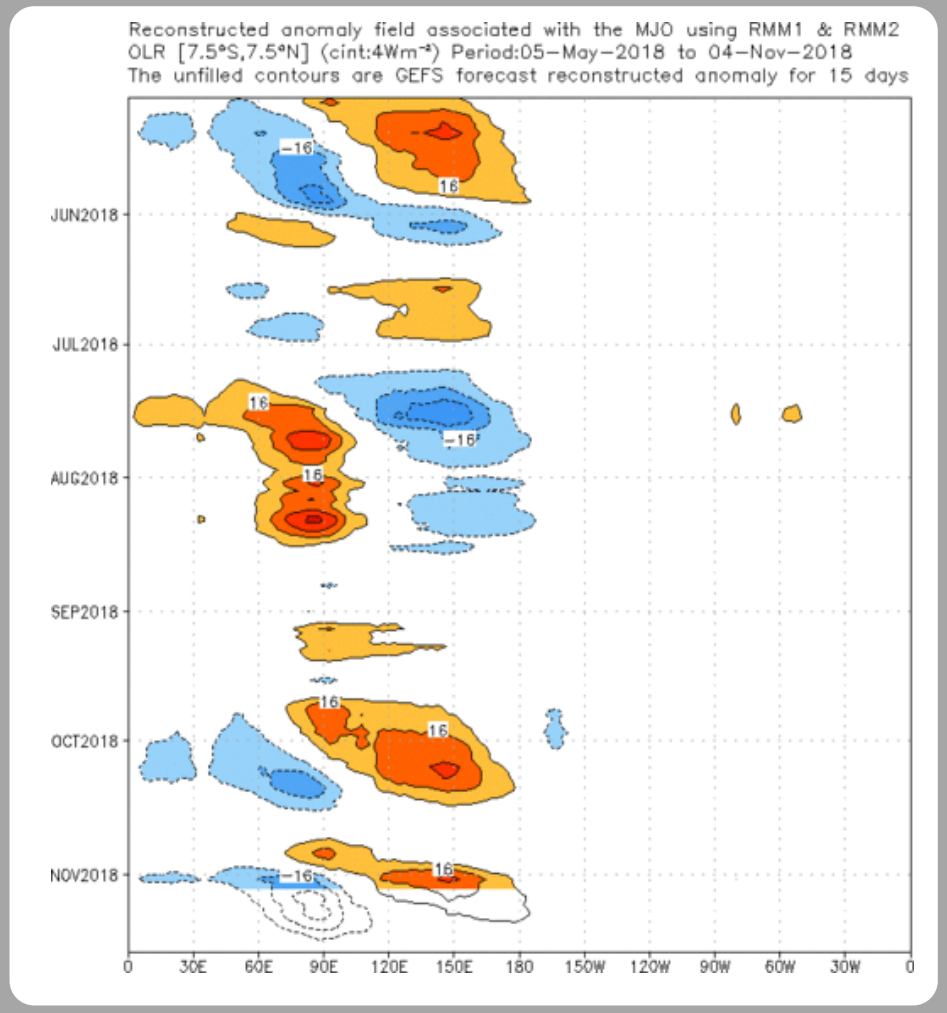

Constructed Analog (CA) MJO Forecast

Figures below show MJO associated OLR anomalies only (reconstructed from RMM1 and RMM2) and do not include contributions from other modes (*i.e.*, ENSO, monsoons, etc.)

Spatial map of OLR anomalies for the next 15 days

Time-longitude section of (7.5° S-7.5° N) OLR anomalies - last 180 days and for the next 15 days

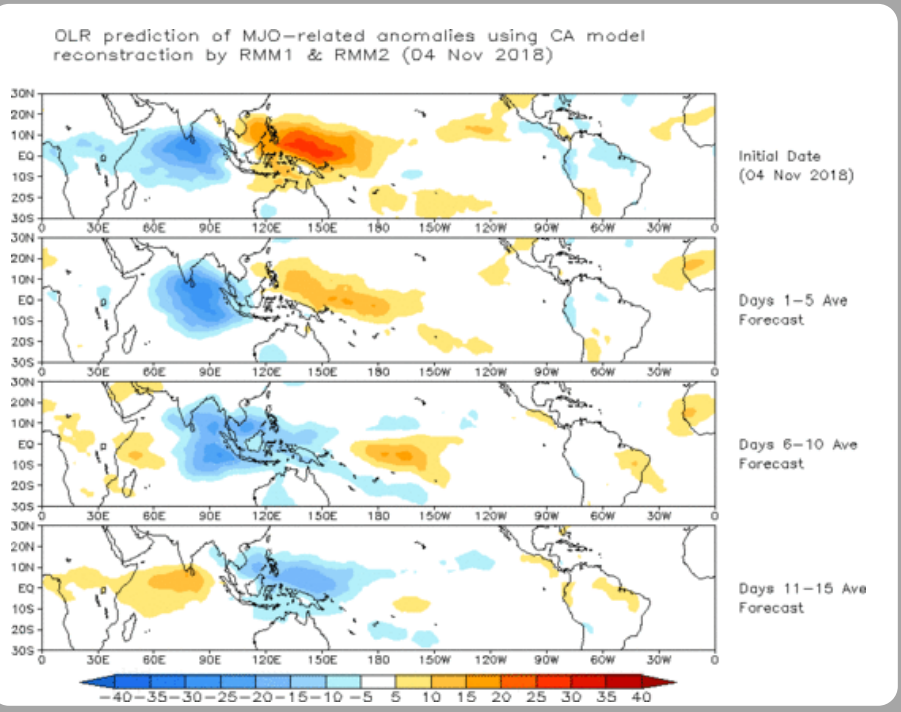

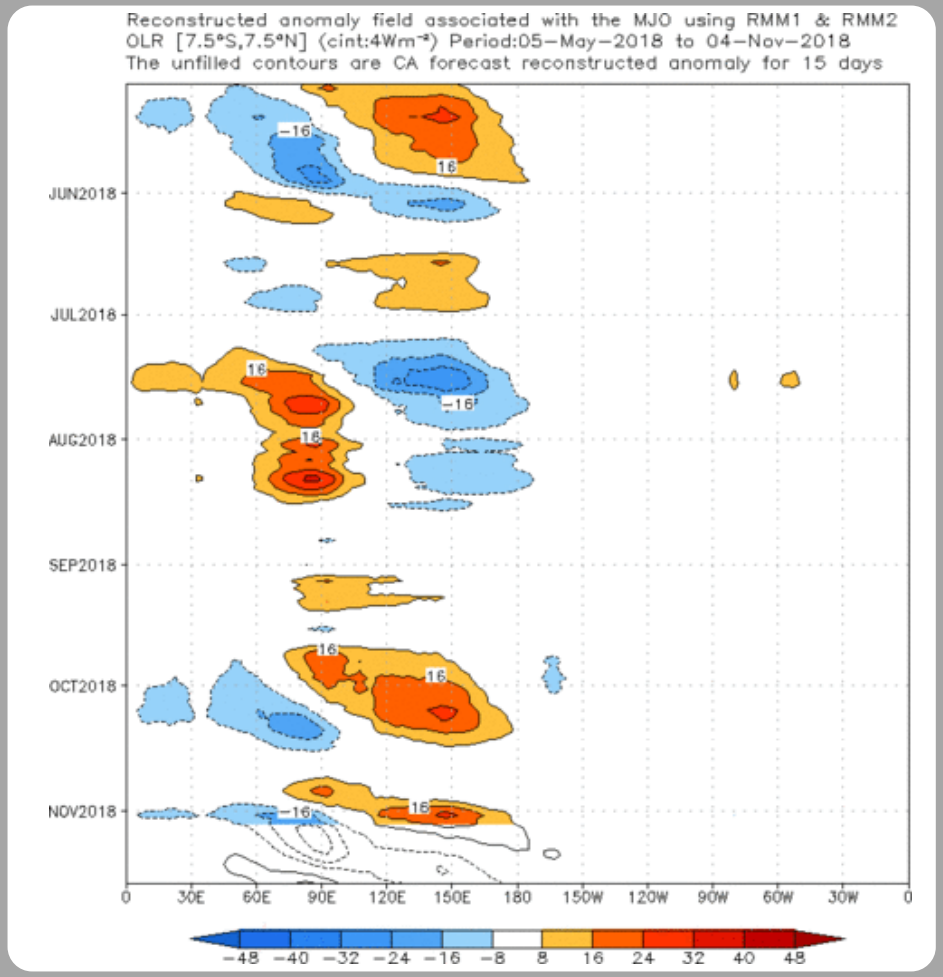

The OLR forecast based on the constructed analog RMM-index forecasts is quite similar to the GEFS spatial pattern of anomalous convection for the first ten days, albeit slightly more progressive. This framework also pushes the active MJO phase into the West Pacific by late in Week-2.

MJO Composites - Global Tropics

850-hPa Velocity Potential and Wind Anomalies (Nov - Mar)

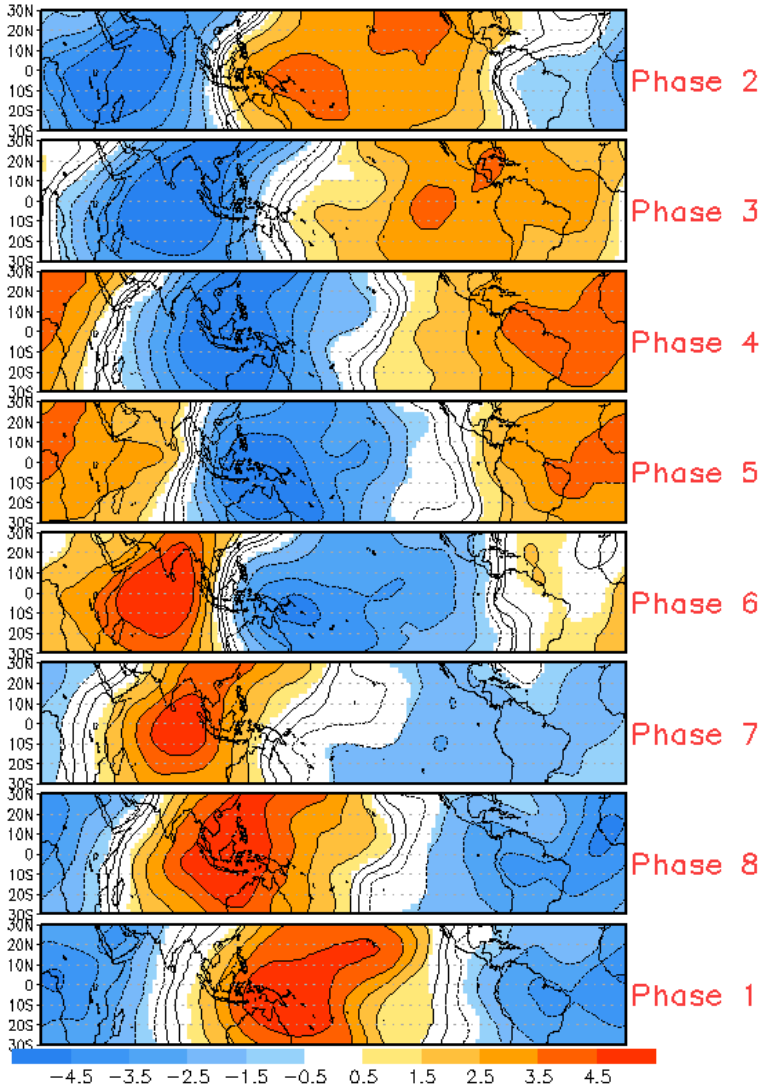

Precipitation Anomalies (Nov - Mar)

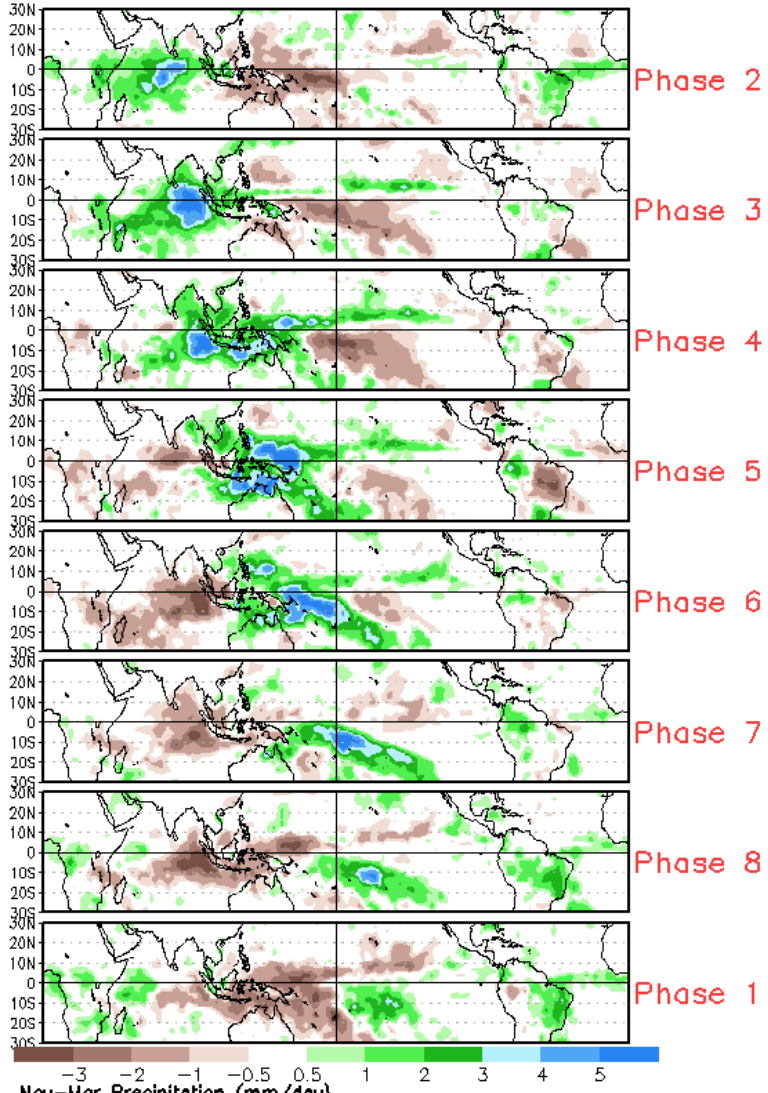

U.S. MJO Composites - Temperature

Left hand side plots show temperature anomalies by MJO phase for MJO events that have occurred over the three month period in the historical record. Blue (orange) shades show negative (positive) anomalies respectively.

Right hand side plots show a measure of significance for the left hand side anomalies. Purple shades indicate areas in which the anomalies are significant at the 95% or better confidence level.

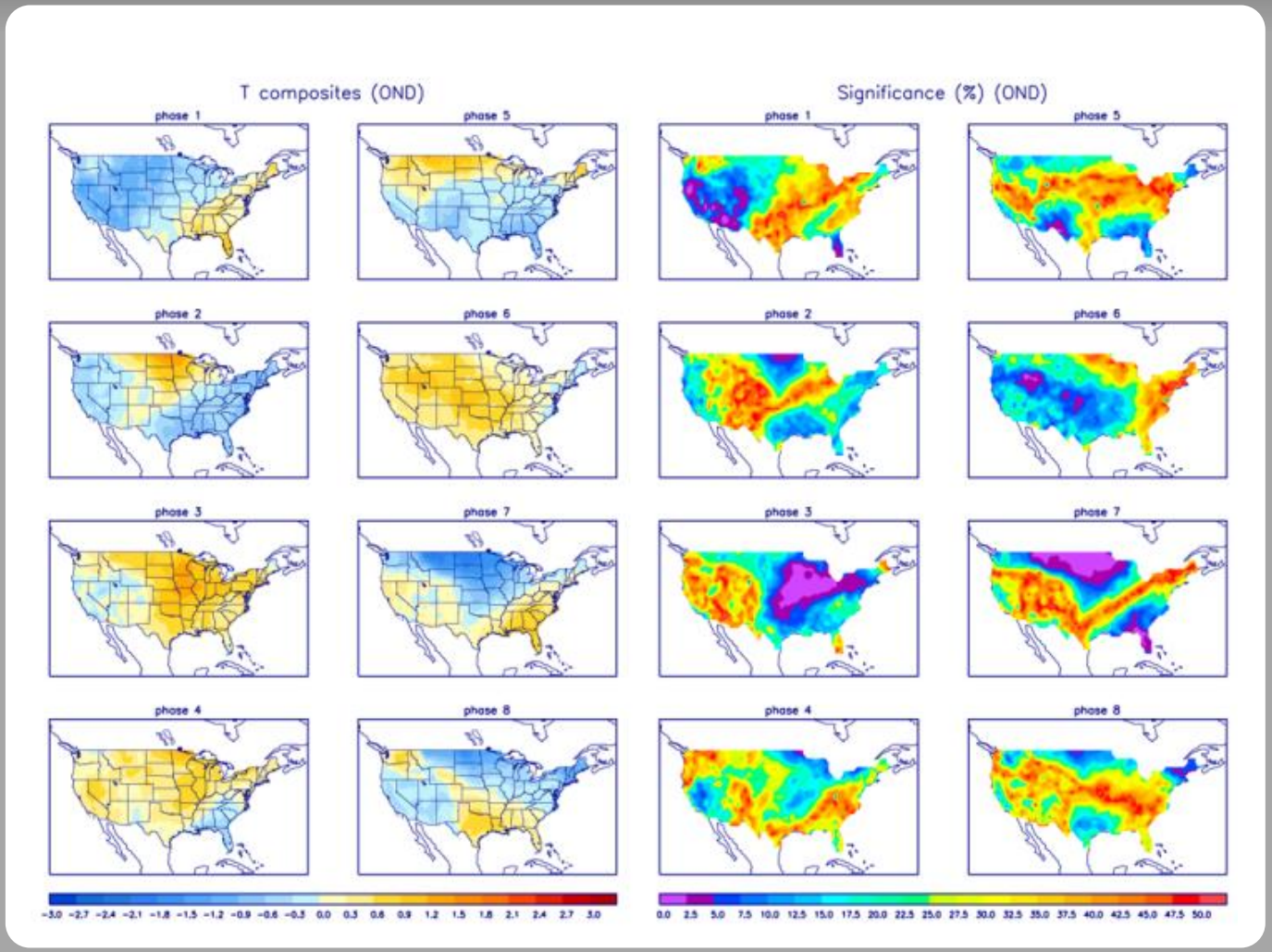

Zhou et al. (2011): A composite study of the MJO influence on the surface air temperature and precipitation over the Continental United States, *Climate Dynamics*, 1-13, doi: 10.1007/s00382-011-1001-9

http://www.cpc.ncep.noaa.gov/products/precip/CWlink/MJO/mjo.shtml

U.S. MJO Composites – Precipitation

Left hand side plots show precipitation anomalies by MJO phase for MJO events that have occurred over the three month period in the historical record. Brown (green) shades show negative (positive) anomalies respectively.

Right hand side plots show a measure of significance for the left hand side anomalies. Purple shades indicate areas in which the anomalies are significant at the 95% or better confidence level.

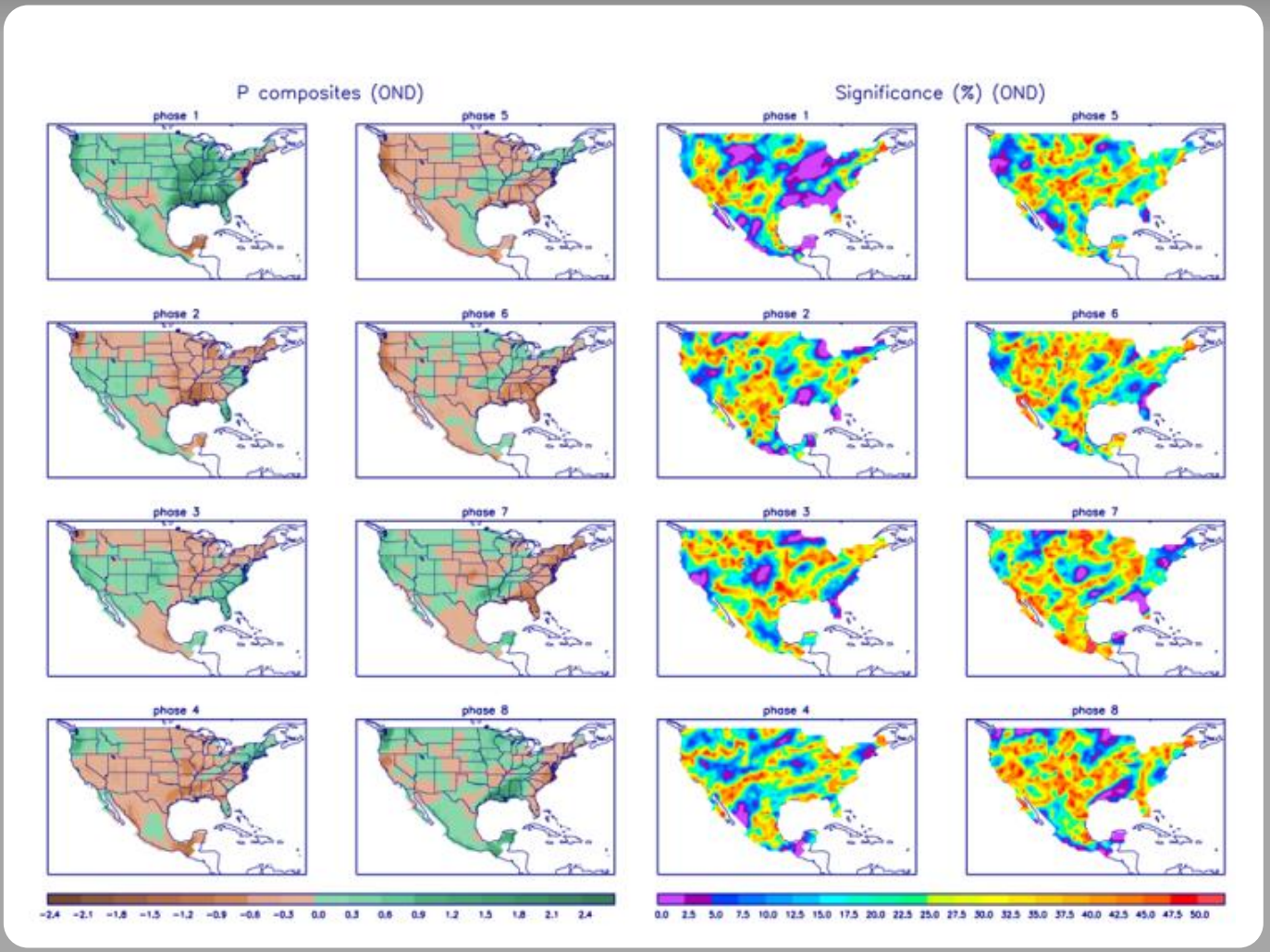

Zhou et al. (2011): A composite study of the MJO influence on the surface air temperature and precipitation over the Continental United States, *Climate Dynamics*, 1-13, doi: 10.1007/s00382-011-1001-9

http://www.cpc.ncep.noaa.gov/products/precip/CWlink/MJO/mjo.shtml